Journal of Geological Society of Sri Lanka Vol. 23- I (2022), 34-54 DOI: http://doi.org/10.4038/jgssl.v23i1.65

METAMORPHIC EVOLUTION OF CHARNOCKITES ACROSS THE INFERRED HIGHLAND-WANNI BOUNDARY IN NORTHEASTERN SRI LANKA

W. M. R. JAYATHILAKE[1], P. L. DHARMAPRIYA[1*], R. KLEINSCHRODT[2], B. SPIERING[3]

[1]*Department of Geology, University of Peradeniya, Sri Lanka*
[2]*Institute for Geology and Mineralogy, University of Cologne, Germany*
[3]*Steinmann Institutfür Geologie, University of Bonn, Germany*

**Corresponding author e-mail: prasannad@sci.pdn.ac.lk*

(Received 25th July 2022; accepted 21st August 2022)

ABSTRACT

Charnockites are hypersthene-bearing granitoids that form a minor but important component of the Earth's lower crust. Charnockite is a common lithology in the Highland Complex (HC) and Wanni Complex (WC) of Sri Lanka. These two Complexes are considered lithotectonic units having two different protolith histories. The northeastern part of the HC and WC is poorly explored compared to the central, southern, and southwestern parts of the two Complexes. In this study for the first time, we have attempted to study the metamorphic evolution of charnockites across the northeastern part of the inferred boundary between the HC and WC studying equilibrium mineral assemblages utilizing conventional and trace element geothermometers. In the WC side, hedenbergite-ferrosilite assemblage in a charnockite can be considered as the preserved relict assemblages of the rock's igneous protolith. Orthopyroxene of the majority of charnockites in both HC and WC is apparently formed during the prograde dehydration of hornblende and biotite. Mineral assemblages and reaction textures of all the charnockites provide evidence for a clockwise pressure-temperature path during late prograde to retrograde evolution. The studied charnockites were metamorphosed from hornblende-granulites to pyroxene-granulite facies conditions with a minimum temperature of around 750- 800 °C. A period of the near-isobaric cooling (IBC) stage after peak metamorphism has been suggested for both HC and WC charnockites. We confirm that there is no evidence for contrasting metamorphic evolution of charnockites across the inferred HC-WC boundary.

Keywords*: Charnockites, Metamorphic evolution, Highland Complex, Wanni Complex, Sri Lanka*

INTRODUCTION

Charnockites are hypersthene-bearing granitoids that form a minor but important component of the Earth's lower crust (Janardhan et al., 1982; Frost and Frost, 2008). Charnockitic rocks form extensive found in many granulite terranes (as orthogneisses) and are less commonly found in unmetamorphosed plutons (Frost and Frost, 2008). Charnockites are typically characterised by the presence of anhydrous minerals including orthopyroxene (or rarely fayalite), clinopyroxene and garnet as major mineral constitutes and limonite, magnetite, zircon, monazite as minor to accessory phases and hydrous mineral phases such as biotite and hornblende as overt printed phases. Hence the mineral phases and assemblages of charnockites can be used for retrieving the Pressure-Temperature-time (*P*-*T*-*t*) evolution of high-grade metamorphic terrains (Frost et al., 1988; Lindsley and Frost, 1992; Frost and Lindsley, 1992).

Sri Lanka is considered a discreet crustal fragment of the Central Gondwana (Shirashi et al. 1994l Santosh et al., 2014). Over 90 % of the basement of the country is composed of high-grade metamorphic rocks. Based on Nd- model ages, U-Pb zircon ages and regional structural interpretations the Precambrian crust of Sri Lanka has been subdivided into four major lithotectonic units (Kröner et al., 1991; Cooray, 1994) shown in Figure 1 named as the Wanni Complex (WC), the Highland Complex (HC), the Vijayan Complex (VC) and the Kadugannawa Complex (KC) (Milisenda et al., 1988, 1994; Kröner et al., 1987, 1991; Kehelpannala, 1991, 2003, 2004, Kleinschrodt et al., 1991; Kriegsman, 1994). The boundary between the HC and the WC is considered an inferred tectonic boundary since it has been solely demarcated using Nd- model ages by Kröner et al. (1991). Later some researchers attempted to refine the boundary after doing structural geological studies in the Central part of the county (Kehelpannala and Ranaweera, 2007; Ranaweera and Kehelpannala, 2019). However, the northeastern part of the HC-WC boundary is poorly explored.

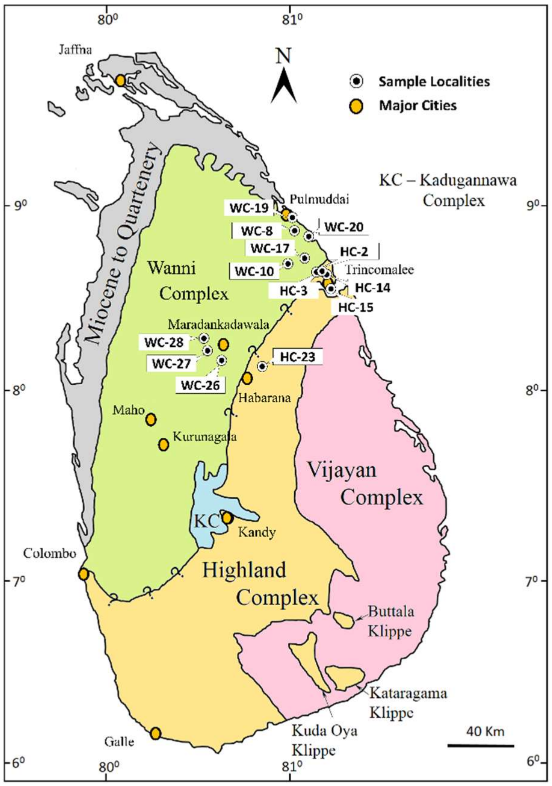

Fig. 1: *Sampling localities concerning the geological subdivisions of Sri Lanka (Litho-tectonic units after Kröner et a., 1991 and Cooray,1994)*

The metamorphic evolution of the HC is well studied using metapelites and psammopelitic gneisses, mafic granulites, calc-silicate gneisses and rarely using charnockites that were collected from mainly in the central part and less commonly in the southwestern and southern part of the Complex. In contrast, there is no attempt made to study the metamorphic evolution of rocks in the northeastern part of the HC. The *P-T* studies on WC is also mainly confined to the central part and the southern-western part of the Complex (Rasse and Schenk, 1994; Hirayama et al., 2020).

Charnockite is one of the dominant lithologies across the northeastern part of the inferred HC-WC tectonic boundary. Our recent geological investigations especially around Trincomalee (e.g. Jayathilaka et al., 2020; our unpublished data) revealed the existence of contrast geochemical chemical affinities of charnockites across the above-mentioned tectonic boundary. In this study first time, we have attempted to study the metamorphic evolution of charnockites across the northeastern part of the inferred boundary between the HC and Wanni Complex WC using equilibrium mineral assemblages and, conventional and trace element geothermometers.

GEOLOGICAL BACKGROUND

The whole-rock Nd isotopic data indicate the rocks in the HC were mainly derived from late Archean to Paleoproterozoic sources (3.2-2 Ga; Milisenda et al., 1988, 1994). The HC is mainly composed of granulitic paragneisses such as garnet sillimanite gneisses, quartzites, marbles and calc-silicates rocks, and orthogneisses of largely granitoid composition and charnockitic rocks (Cooray, 1994). The HC has been interpreted as a tilted crustal section and across the Complex, the metamorphic temperatures and pressures increase from 600-850 °C and 5-7 kbar in the southwest to 800-900 °C and 8-10 kbar in the central part and towards the east (Kröner and Williams, 1993; Raase and Schenk, 1994; Dharmapriya et al., 2014; 2017). Ultra-high temperature (UHT) granulites (which have experienced extreme crustal metamorphism at 900-1150 °C and 9 - 12.5kbar) have been reported at a few localities in the central HC and rarely from the south-western part of HC (Kriegsman and Schumacher, 1999; Osanai et al., 2006; Sajeev and Osanai, 2004a, 2004b; Sajeev et al., 2007, Dharmapriya et al. 2015, 2021). The emplacement of the protolith of the orthogneisses of the HC occurred mainly in three episodes of around 1950 - 1800 Ma, 850 - 670 Ma and ~580 Ma (Kröner and Jeckel, 1993; Hölzl et al., 1994; Sajeev et al., 2007; Kitano et al., 2018; He et al., 2019). The peak granulite facies metamorphism of the Complex was suggested to occur around 610 - 530 Ma (e.g. Kröner et al., 1987, Hölzl et al., 1991, 1994; Sanjeev et al., 2010; Dharmapriya et al., 2015b, 2016; Takamura et al., 2016; Kitano et al. 2018). According to previous studies on the *P-T* evolution of the HC, which reported sillimanite both as inclusion and as a matrix mineral in garnet-bearing metapelites, the equilibration at peak T occurred in the sillimanite field (e.g. Perera, 1987, Perera, 1994, Hiroi et al., 1994, Raase and Schenk, 1994, Dharmapriya 2017). Since the occurrences of relict kyanite andstaurolite as inclusions in porphyroblastic garnet in sillimanite-bearing metapelites (Hiroi et al., 1994, Raase and Schenk, 1994; Dharmapriya et al., 2017), most of the workers suggested a clockwise *P–T* trajectory for the HC granulites.

The WC yields Nd-model ages of 2000 – 1000 Ma (Milisenda et al. 1988, 1994). The WC is composed of a range of granitic, granodiorite, monzonite, tonalite, charnockitic and enderbitic rock compositions as varying chemistry of protoliths (Pohl and Emmermann, 1991). The western part of WC consists of less deformed granites including unmetamorphosed post-tectonic K-feldspar-rich granite of Thonigala (Hölzl et al, 1991; Cooray 1994). The peak metamorphic conditions of the WC have been suggested to be 700-830 ^{0}C and 5-7kbar (Raase and Schenk, 1994; Santosh et al., 2014; Hirayama et al., 2020). The intrusion ages of Wanni gneisses mainly are around 1100 - 920 Ma, 800 - 750 Ma and around 580 Ma (Kröner et al., 1994; 2003; Hölzl et al, 1994; Santosh et al., 2014; He et al., 2016). Peak metamorphism had happened around 590 - 540 Ma (Kröner et al., 1994; 2003; Hölzl et al, 1994; Santosh et al., 2014; He et al., 2016).

The currently accepted boundary between HC-WC was determined by Kröner et al., (1991) after considering the lithologies and structural besides Nd modal ages (after Milisenda et al., 1988), Pb isotopic discriminations (after Lew et al., 1991) and U-Pb zircon ages of metaigneous and metasedimentary rocks (Hölzl et al., 1991). However, due to a lack of sufficient geological information from geochemical, geochronological, structural and petrological studies, the position of the southwestern and the northeastern HC-WC boundary is still controversial. The inferred tectonic boundary of the HC-WC from the northern part of Kandy to Habarana (Fig. 1), the boundary in the central part of the country has more or less been fixed in history (Kehelpannala and Ranaweera, 2007; Ranaweera and Kehelpannala, 2019). Based on structural geology-related studies, some workers interpreted the HC-WC boundary as a lower crustal ductile shear zone (Kehelpannala, 1997; Ranaweera and Kehelpannala, 2019).

Fig. 2: *Representative field photographs charnockites in the study area a) a massive charnockite at HC-2, b), charnockitic gneiss at HC-3, c) and d) a massive charnockite at WC-26 and WC-28*

In contrast, the northeast part of the boundary between the two Complexes is highly uncertain and the nature of the boundary in the region has not yet been understood.

The KC crops out in doubly plunging upright folds around Kandy in the central part of the country, formerly known as "Arenas" (Vitanage, 1972; Almond, 1991) and yields Nd-model ages ranging between 1800-1100 Ma (Milisenda et al., 1988 and 1994). The dominantly upper amphibolite facies VC yields Nd-model ages are in the range of 3300-1100 Ma (Milisenda et al., 1988; 1994; Malaviarachchi et al., 2021). This Complex mainly consists of microcline-bearing granitic gneisses, augen-gneisses, migmatites and hornblende-biotite gneisses (Cooray, 1984; Kehelpannala, 1997; Mathavan et al., 1998; Kröner et al., 2013).

SAMPLE DESCRIPTIONS

Fresh charnockites samples were collected from quarries and road cuts (Table 1) from two separate traverses across the inferred boundary of HC-WC. Traverse 1 extended from Trincomalee to Pulmuddai and Travers 2 from Habarana to Maradankadawala (Fig. 1). Charnockites in sampling localities are massive and show the typical greasy lustre (Fig. 2a, b, c, d). Quartz, two feldspars, and orthopyroxene are frequently present as major mineral constituents. Occasionally biotite (at localities WC-8, WC-10, WC-17, WC-19, WC-20, WC-26, WC-27) and garnet (at localities WC-19, WC-20) are also present as major mineral phases. At localities HC-3 and HC-14, hornblende and clinopyroxene were found as major mineral phases.

***Table 1**: GPS co-ordinates of charnockite localities*

Sample No.	GPS Co-ordinates	
	Latitude	Longitude
H-W-2	8.622992	81.16084
H-W-3	8.622891	81.15989
H-W-8	8.847851	81.01219
H-W-10	8.720435	80.95698
H-W-14	8.60132	81.18567
H-W-15	8.51371	81.20856
H-W-17	8.67894	81.06889
H-W-19	8.92382	80.99850
H-W-20	8.81322	81.09378
H-W-23	8.053506	80.83359
H-W-26	8.097182	80.61638
H-W-27	8.151971	80.53283
H-W-28	8.229421	80.52283

PETROGRAPHY AND TEXTURAL EVOLUTION

Charnockites in the Highland Complex side from the inferred HC-WC boundary

Hereafter, this paper collected charnockites from the Highland Complex-side with respect to the inferred HC-WC boundary, after Kröner et al., (1991) is referred to as "CHCs" (Charnockite-Highland Complex Side). These charnockites are mainly composed of quartz, alkali feldspar, plagioclase, orthopyroxene, clinopyroxene, hornblende as well as primary biotite grains found in a few locations (HC-3). Also, opaque (ore) minerals are present in high modal percentages in most sampled localities (HC-3, HC-14, HC-15). Overall average percentages are slightly varied from sample to sample. Minor minerals and accessories are zircon, and ore minerals (mainly ilmenite, and magnetite). Apatite is present as an accessory phase with uneven distribution (HC-21, HC-15). Secondary hornblende, biotite and chlorite are found in some samples (HC-15, HC-21).

The matrix of almost all samples are composed of subidioblastic and xenoblastic fine to medium quartz, alkali feldspar, and plagioclase showing interlobate texture as shown in Fig. 3a in locations of HC-14, HC-15 and HC-21. Granoblastic texture was also identified at a few locations (HC-2, HC-3) (Fig. 3b). Subidioblastic porphyroblasts of mafic minerals are common in the matrix showing sharp and uneven dissolved contacts and are uniformly distributed (HC-3, HC-14, HC-15). Occasionally, grains are present as cumulative texture whereas gathering of two pyroxenes and hornblende (HC-2, HC-21). Foliation is demarcated by mafic minerals rather than felsic minerals. These grains are elongated and relict grain aggregates (HC-2, HC-21). The following assemblages are supposed to be dominant under peak metamorphic conditions: Opx + Cpx + Hbl + Kfs + Pl + Qz + Ilm, Opx + Cpx + Kfs+ Pl + Qz + Ilm ± Hbl, and Opx + Cpx + Hbl + Kfs + Pl +Qz + Ilm ± Bt

CHCs preserved evidence for the following reactions. Hornblende-quartz coexisting inclusions observed in clinopyroxene grain that are associated with orthopyroxene and plagioclase (Fig. 3c). Quartz inclusions observed in many samples (HC-14) usually in the rim area than core in clinopyroxene porphyroblasts. Also both biotite and hornblende were found as inclusions (Fig. 3d)

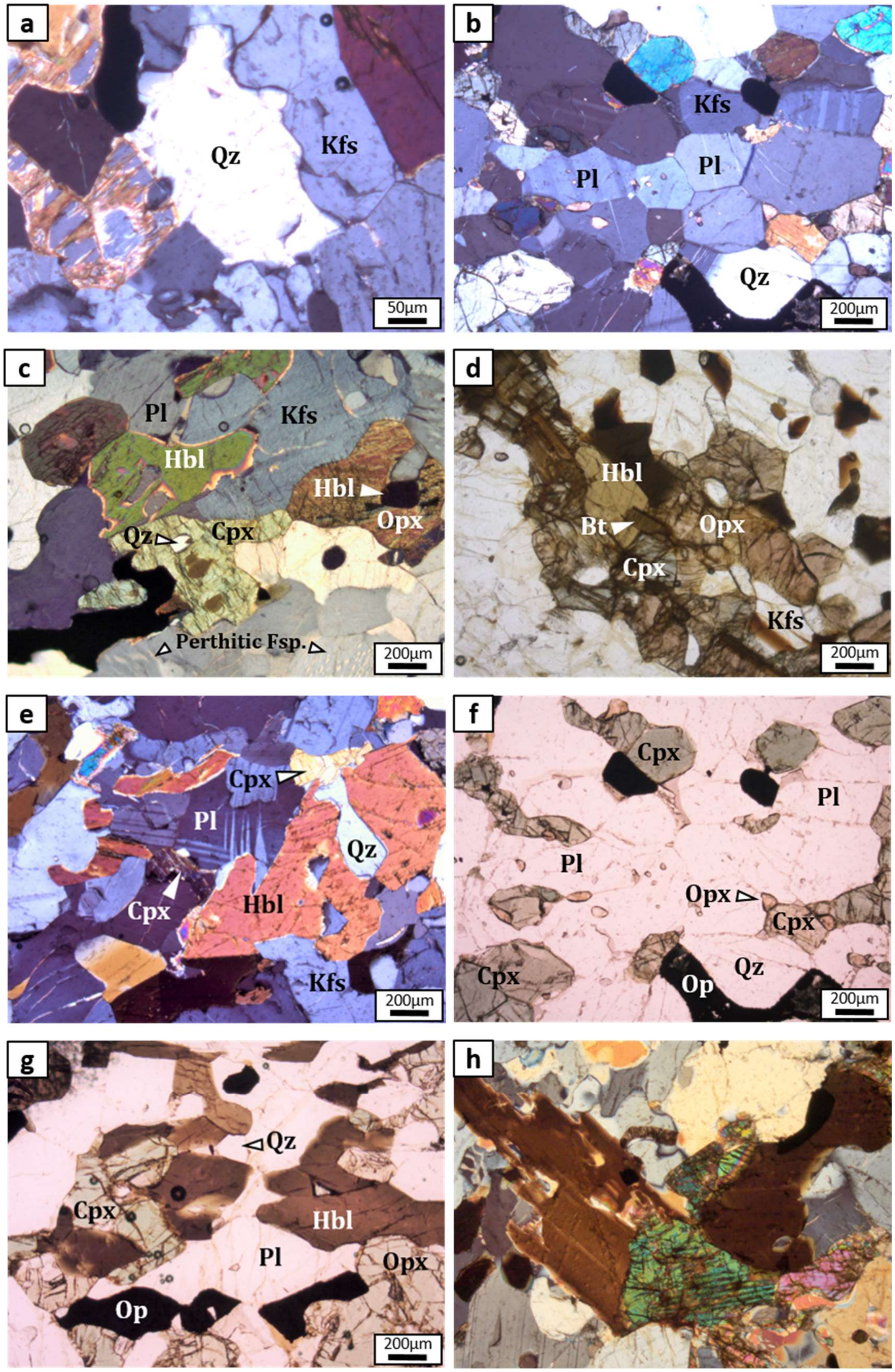
a
Qz
Kfs
50µm
b
Kfs
Pl
Pl
Qz
200µm
c
Pl
Kfs
Hbl
Hbl
Opx
Qz
Cpx
Perthitic Fsp.
200µm
d
Hbl
Bt
Opx
Cpx
Kfs
200µm
e
Cpx
Pl
Qz
Cpx
Hbl
Kfs
200µm
f
Cpx
Pl
Pl
Opx
Cpx
Cpx
Op
Qz
200µm
g
Qz
Cpx
Hbl
Pl
Opx
Op
200µm
h

Continued

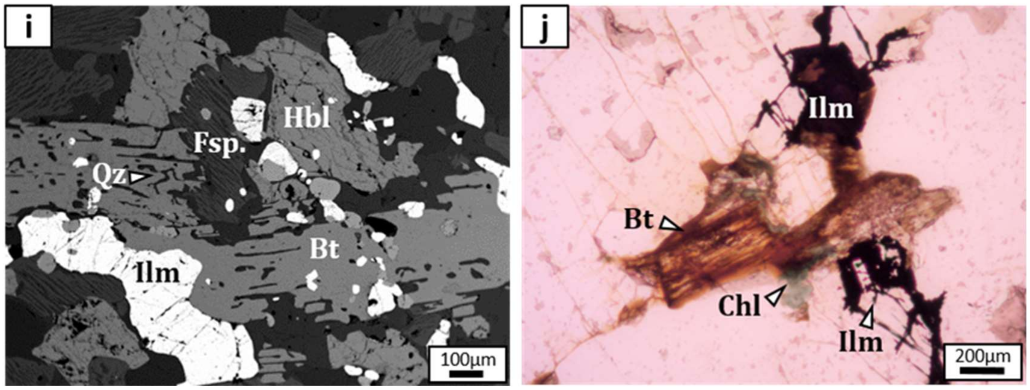

Fig. 3: *Representative photomicrographs showing metamorphic reactions and textures in HC charnockite samples (a) interlobate texture (HC-21) (b) granoblastic texture (HC-2), (c) HC-14 showing reaction 1, (d) HC-21 showing reaction 2, (e) HC-3 indicating reaction 3 (f) HC-2 showing reaction 4 (g) HC-2 reaction 5 (h) HC-3 indicating reaction 7 (i) HC-2 skeletal biotite in reaction 8 (j) HC-3 showing Opx alteration with forming secondary Bt and furcate distribution of ilmenite*

in pyroxenes (H-W-21). Hence the possible dehydration reactions are:

Hbl + Qz → Cpx + Opx + Pl + V ---------------- (1)

Bt + Hbl + Qz → Cpx + Opx + Pl + Kfs + V --- (2)

Formation of relatively small xenomorphic clinopyroxene around hypidiomorphic hornblende grains which have coexisted with plagioclase (Fig. 3e) indicating the dehydration reaction:

Hbl + Qz → Cpx + Pl + V ----------------------- (3)

Almost all of the samples represent the equilibrium of clinopyroxene and orthopyroxene with sharp grain boundaries. Samples having hornblende also represent sharp grain margins between plagioclase and hornblende (Fig. 3c).

Fine-grained orthopyroxene along the grain boundary is relatively coarse-grained clinopyroxene under quartz and plagioclase (Fig. 3f) representing the solid-solid net transfer reaction:

Cpx + Qz → Opx + Pl + Ilm --------------------- (4)

Breakdown of orthopyroxene and clinopyroxene into hornblende and ore minerals properly identified in rocks (HC-2) (Fig. 3g) possible through the hydration reaction:

Opx + Cpx + Pl + V → Hbl + Qz + Ilm --------- (5)

Overprinting of hornblende after clinopyroxene under the presence of plagioclase could indicate the hydration reaction:

Cpx + Pl + V → Hbl + Qz + Opaque-------------- (6)

Those grains are in contact with plagioclase and quartz in the matrix and some hornblende grains are developed in encountering plagioclase and quartz as inclusions. Occasionally, overprinted hornblende and biotite (Fig. 3h) after clinopyroxene in samples (HC-3) indicates the dehydration reaction:

Cpx + Pl + Kfs + V → Hbl + Bt + Qz + Ilm----- (7)

The hornblende-biotite gneiss associated with the HC-2 contains skeletal biotite, plagioclase, quartz intergrowths (Fig. 3i) after hypidiomorphic to xenomorphic hornblende and xenomorphic perthitic feldspar (Perthitic Fld.) indicating the reaction:

Hbl + Perthitic Fld. ± V → Bt +Pl + Qz --------- (8)

The secondary biotite and chlorite have resulted from alteration of two pyroxenes which were found along the cleavage planes (Fig. 3j) or as an almost replaced pyroxene grain. As well as the furcate distribution of ilmenite (Fig. 3j) observed in some sections. The radial arrangement of secondary biotite flakes around opaque minerals is commonly recognized. These kinds of reactions indicate shallow cooling aqueous conditions (e.g. Sajeev and Osanai, 2004).

Perthitic texture was found at some locations consisting of albite lamellae (Fig. 4c) in plagioclase and microcline in Kfs (HC-14, HC-15). Coarse to fine grains of plagioclase with mechanical deformation twinning and tapering edges can be identified in HC-3. Stretching quartz was observed in HC-2.

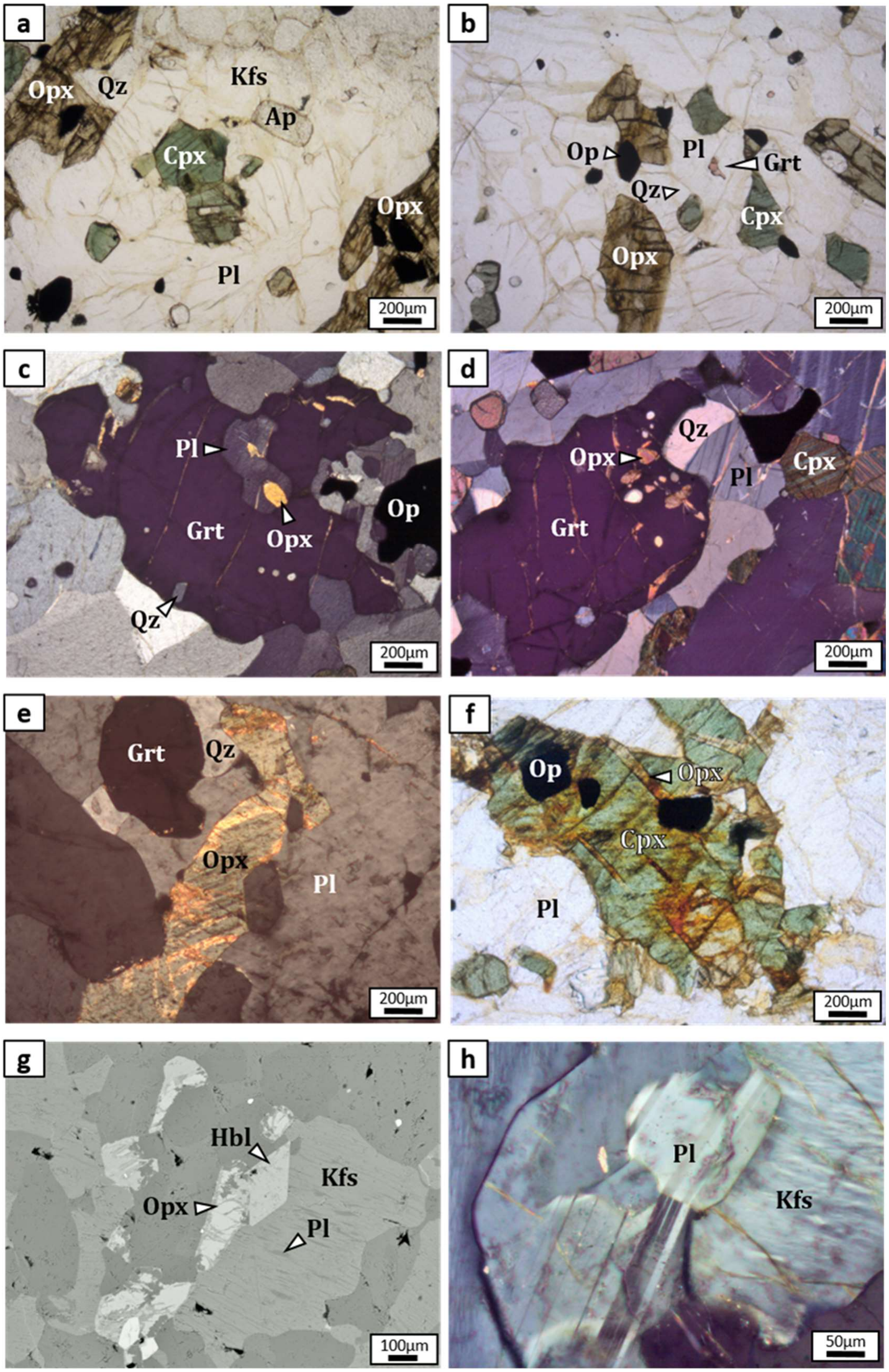

Fig. 4: Representative photomicrographs in WC charnockite samples (a) xenoblastic porphyroblasts of clinopyroxene (WC-17), (b) WC-17 showing reaction 9 (c) and (d) WC-20 showing reaction 10, (e) WC-10 showing reaction 10 (f) WC-27 indicating exsolved pyroxene (g) exsolved pyroxene grain in WC-27, (g) perthitic to mesoperthitic texture in WC-8 and (h) mechanical twinning of Pl showing twin defects in WC-8

Charnockites in the Wanni Complex Side from the Inferred HC-WC boundary

Hereafter, this paper collected charnockites from the Wanni Complex-side with respect to the Inferred HC-WC boundary after Kröner et al., (1991) is referred to as "CWCs" (Charnockite-Wanni Complex Side). These charnockites consist of quartz, alkali feldspar, plagioclase, orthopyroxene grains and opaque minerals (mainly ilmenite and magnetite) as minor mineral phases. Occasionally clinopyroxene and hornblende are also present. In a few localities (WC-19, WC-20) charnockites contain garnet. Allanite, apatite and zircons are common accessory minerals in most samples. Hornblende and biotite frequently occur as overprinted products after pyroxenes.

Most of the constituent mineral grains show medium to fine grain size (3mm-0.2mm) distribution. Some samples are composed of very fine grains with considerable grain size variation (WC-27, WC-28). Subidioblastic to xenoblastic interlobate matrix grains are dominant in most of the samples and otherwise coarse-grained irregular shape xenoblastic grains are found in some localities (WC-8, WC-26). Xenoblastic porphyroclasts of clinopyroxene, hornblende, and orthopyroxene, show sharp cleavages (Fig. 4a) which have slightly disappeared due to later alterations. These grains are not where the mafic minerals are accumulated (WC-10, WC-26, WC-27, WC-28). Foliation is defined by both elongated mafic minerals of clinopyroxene, hornblende and orthopyroxene and biotite and felsic minerals of quartz, alkali feldspar and plagioclase (WC-10, WC-17, WC-28) except few samples. Some other samples show orthopyroxene and clinopyroxene preferred orientation (WC-8, WC-26).

The following minerals assemblages seemed to exist as peak metamorphic assemblages in WC charnockites: Opx + Cpx + Kfs + Pl + Qz + Ilm, Opx + Hbl + Kfs + Pl + Qz + Ilm, Opx + Cpx + Grt + Kfs + Pl +Qz+ Ilm, Opx + Grt + Kfs + Pl + Qz + Ilm.

CWCs shows the following textural have been identified during the petrographic study. Tiny xenomorphic grains of garnet were found as inclusions in some medium to coarse-grained hypidiomorphic plagioclase (Fig. 4b) which are surrounded by two pyroxenes and opaque minerals in some of CWCs charnockites. Occasionally, relict quartz inclusions are present in those orthopyroxene grains and plagioclase (WC-17, WC-19, WC-28). Above textural features indicate the reaction:

$$\text{Cpx+Grt} \rightarrow \text{Opx+Qz+Pl+ Opaque} \text{ ---------------- } (9)$$

In location, WC-20 has respectively large grains of garnet with coexisting inclusions of orthopyroxene and plagioclase near the rim and also all of the quartz included in garnet grains has been limited to rim area (Fig. 4c, d).

The reaction should be,

$$\text{Opx + Pl} \rightarrow \text{Grt + Qz} \text{ ----------------------------- } (10)$$

The formation of tiny grains of retrograde garnets around the orthopyroxene are associated with plagioclase and quartz in WC-10 (Fig. 4e). Newly formed quartz grains do not show more deformation than early existing grains as. Also, the lack of wavy extinction suggests that the reaction is similar to the reaction (10).

Exsolved orthopyroxene lamellae in clinopyroxene are observed in location WC-27 (Fig. 4f), Perthitic to mesoperthitic textures (Fig. 4g) are common in most samples (WC-8, WC-17, WC-26). Mechanical twinning of plagioclase (Fig. 4h) and the twin defects show the deformational characteristic features (WC-8, WC-19).

MINERAL CHEMISTRY

Mineral compositions of both CHCs (for two samples: HC-2, HC-3) and CWCs (for two samples: WC-8, WC-10) were analysed using two-electron microprobes analysers (EPMA) installed at the University of Cologne, and the University of Bonn in Germany. At the University of Cologne, analyses were carried out under JEOL electron probe microanalyzer (EPMA) and all analyses were operated at an accelerating voltage of 20 kV and 10 nA beam current, 3 μm beam spot and 10-30 s counting time on peak. The precision of all analyzed elements are better than 98.5%. At the University of Bonn, analyses were carried out under JEOL 733 electron probe microanalyzer (EPMA) installed at the University of Bonn, Germany. All analyses were operated at an accelerating voltage of 20 kV and 10 nA beam current, 3 μm beam spot and 10-30 s counting time on peak. The precision of all analysed elements are better than 98.5%. Tables 2, 3, 4 and 5 represent mineral compositions of samples HC-2, HC-3, WC-8 and WC-10 respectively.

Table 2: *Representative Electron Microscope Analysis of minerals in HC-2*

Mineral	**Clinopyroxene**		**Hornblende**		**Biotite**		**Magnetite**		**Ilmenite**		**Plagioclase**		**Alkali-feldspar**	
	core	**rim**	**core**	**rim**	**core**	**rim**	**core**	**rim**	**core**	**rim**	**core**	**rim**	**core**	**rim**
SiO_2	49.28	49.85	39.87	39.83	36.5	37.07	5.02	bdl	bdl	bdl	58.39	57.82	64.92	65.01
TiO_2	0.65	0.46	2.77	2.64	4.07	4.05	0.17	1.28	52.07	53.18	0.03	bdl	0.05	0.01
Al_2O_3	4.32	3.55	12.82	12.85	16.40	16.19	1.47	0.34	bdl	0.02	27.59	28	19.3	19.64
Cr_2O_3	0.02	0.06	0.06	0.04	0.05	bdl	0.11	0.11	bdl	0.04	bdl	0.03	0.03	bdl
FeO	12.36	11.38	19.01	18.55	15.04	15.09	86.53	96.09	44.62	43.95	0.18	0.31	0.11	0.1
MnO	0.34	0.34	0.25	0.27	0.19	0.17	0.07	0.06	3.17	3.15	0.03	bdl	bdl	0.05
MgO	10.36	11.06	8.92	8.63	13.82	13.99	1.58	0.01	0.37	0.33	0.01	bdl	0.01	bdl
CaO	22.21	22.64	11.89	11.77	0.04	0.04	0.09	0.06	0.03	0.05	8.34	8.52	0.02	0.01
Na_2O	0.94	0.80	1.87	2.01	0.09	0.06	0.05	bdl	0.04	0.05	6.36	6.56	1.23	1.12
K_2O	0.01	0.01	2.11	2.16	10.33	10.32	0.08	0.01	bdl	bdl	0.39	0.28	15.31	15.6
Total	100.49	100.15	99.55	98.74	96.53	96.99	95.16	97.95	100.2	100.78	101.32	101.51	100.99	101.53
O	6	6	24	24	22	22	4	4	3	3	8	8	8	8
Si	1.872	1.892	6.299	6.334	5.418	5.468	0.228	bdl	bdl	bdl	2.579	2.554	2.965	2.956
Ti	0.019	0.013	0.329	0.315	0.454	0.449	0.006	0.046	0.988	0.999	0.001	bdl	0.002	bdl
Al	0.194	0.159	2.387	2.408	2.869	2.815	0.079	0.019	bdl	0.001	1.436	1.458	1.039	1.053
Cr	0.001	0.002	0.007	0.005	0.006	bdl	0.004	0.004	bdl	0.001	bdl	0.001	0.001	bdl
Fe	0.393	0.361	2.512	2.467	1.866	1.862	3.29	3.866	0.941	0.918	0.007	0.012	0.004	0.004
Mn	0.011	0.011	0.033	0.036	0.024	0.021	0.003	0.002	0.068	0.067	0.001	bdl	bdl	0.002
Mg	0.586	0.626	2.099	2.044	3.056	3.074	0.107	0.001	0.014	0.012	0.001	bdl	0.001	bdl
Ca	0.904	0.921	2.013	2.006	0.006	0.007	0.004	0.003	0.001	0.001	0.395	0.403	0.001	0.001
Na	0.069	0.059	0.572	0.619	0.026	0.018	0.004	bdl	0.002	0.002	0.545	0.562	0.109	0.099
K	bdl	0.001	0.426	0.438	1.957	1.942	0.004	bdl	bdl	bdl	0.022	0.016	0.892	0.905
Total cation	4.047	4.044	16.675	16.673	15.682	15.656	3.729	3.942	2.013	2.001	4.986	5.005	5.014	5.019
An											0.411	0.411	0.001	0.001
Ab											0.567	0.573	0.109	0.098
Or											0.023	0.016	0.89	0.901
Fe^{3+}	0.14	0.131	0.971	0.968										
Fe^{2+}	0.252	0.23	1.541	1.499										
X_{Mg}	0.599	0.634	0.455	0.453	0.621	0.623	0.031	0.001	0.015	0.013				

bdl-below detection limit

Table 3: *Representative Electron Microscope Analysis of minerals in HC-3*

Mineral	Orthopyroxenee		Clinopyroxene		secondary Biotite		Biotite		Hornblende		Plagioclase		Alkali-feldspar	
	rim	core	rim	core	core	rim		rim	core	rim	core	rim	core	rim
SiO_2	51.60	50.89	50.92	51.48	37.87	38.29	36.48	36.47	42.21	41.87	60.66	60.91	61.17	60.55
TiO_2	0.07	0.12	0.19	0.15	3.22	2.83	4.19	4.54	2.61	2.46	bdl	0.03	0.04	0.02
Al_2O_3	0.52	0.60	1.60	1.45	13.67	13.00	13.92	13.84	10.57	10.33	23.92	24.13	23.94	24.04
Cr_2O_3	0.03	bdl	bdl	0.02	0.02	bdl	0.02	0.07	bdl	bdl	0.03	bdl	bdl	bdl
FeO	29.97	29.7	12.68	12.63	18.2	18.85	19.97	19.99	18.67	18.62	0.11	0.12	0.02	0.10
MnO	1.12	1.29	0.48	0.46	0.09	0.09	0.09	0.20	0.36	0.30	bdl	bdl	bdl	bdl
MgO	15.13	14.85	10.54	10.41	11.84	11.96	10.52	10.5	8.52	8.45	0.01	0.01	0.01	bdl
CaO	0.70	0.75	20.96	20.807	0.09	0.17	bdl	0.01	11.07	11.03	5.75	5.74	5.67	5.80
Na_2O	bdl	bdl	0.58	0.58	0.03	0.12	0.08	0.05	1.64	1.71	8.16	8.11	8.28	8.38
K_2O	0.01	0.01	bdl	bdl	9.63	8.73	9.95	9.93	1.44	1.45	0.2	0.19	0.33	0.31
Total	99.14	98.2	97.95	98.04	94.66	94.02	95.21	95.59	97.09	96.22	98.84	99.22	99.45	99.21
O	6	6	6	6	22	22	22	22	24	24	8	8	8	8
Si	2.016	2.01	1.975	1.991	5.786	5.877	5.621	5.601	6.752	6.766	2.727	2.726	2.733	2.717
Ti	0.002	0.004	0.006	0.004	0.37	0.327	0.486	0.525	0.313	0.299	bdl	0.001	0.001	0.001
Al	0.024	0.028	0.073	0.066	2.462	2.352	2.528	2.505	1.994	1.968	1.268	1.273	1.261	1.272
Cr	0.001	bdl	bdl	bdl	0.003	bdl	0.002	0.009	bdl	bdl	0.001	bdl	bdl	bdl
Fe	0.979	0.981	0.411	0.409	2.326	2.419	2.573	2.567	2.498	2.517	0.004	0.004	0.001	0.004
Mn	0.037	0.043	0.016	0.015	0.011	0.011	0.012	0.025	0.049	0.042	bdl	bdl	bdl	bdl
Mg	0.881	0.874	0.609	0.6	2.695	2.735	2.416	2.402	2.032	2.034	bdl	bdl	bdl	bdl
Ca	0.029	0.032	0.871	0.865	0.015	0.028	bdl	0.002	1.898	1.91	0.277	0.275	0.271	0.279
Na	bdl	bdl	0.044	0.043	0.009	0.036	0.025	0.015	0.508	0.535	0.711	0.703	0.717	0.729
K	bdl	bdl	bdl	bdl	1.876	1.709	1.956	1.946	0.294	0.299	0.012	0.011	0.019	0.018
Total cation	3.97	3.972	4.005	3.993	15.554	15.493	15.618	15.597	16.339	16.368	5	4.994	5.004	5.019
An											0.277	0.278	0.269	0.272
Ab											0.711	0.711	0.712	0.711
Or											0.012	0.011	0.019	0.017
Fe3+	0.000	0.00	0.014	0.00	1.368	1.28								
Fe2+	0.9709	0.981	0.397	0.409	0.957	1.139								
X_{Mg}	0.474	0.471	0.597	0.595	0.5307	0.531	0.484	0.483	0.449	0.447				

bdl-below detection limit

Table 4: *Representative Electron Microscope Analysis of minerals in WC-8*

Mineral	Orthopyroxene		Hornblende		Ilmenite		Plagioclase		Alkali-feldspar	
	core	**rim**	**core**	**rim**	**core**	**rim**	**core**	**rim**	**core**	**rim**
SiO_2	47.94	47.22	41.50	40.93	bdl	0.05	63.53	64.35	65.44	65.20
TiO_2	0.12	0.15	1.32	1.38	49.91	49.86	0.01	0.03	bdl	0.04
Al_2O_3	0.28	0.23	9.28	9.39	0.02	bdl	21.83	22.59	18.71	18.87
Cr_2O_3	0.05	0.04	bdl	0.02	0.05	bdl	bdl	bdl	bdl	bdl
FeO	45.57	44.18	28.17	28.32	50.85	49.90	0.05	0.10	0.06	bdl
MnO	0.73	0.87	0.23	0.18	0.26	0.30	0.02	0.01	bdl	bdl
MgO	5.24	5.24	4.25	4.07	0.02	bdl	bdl	bdl	bdl	bdl
CaO	0.87	0.75	10.35	10.24	0.02	0.01	3.79	3.71	0.09	0.12
Na_2O	bdl	0.05	1.97	1.93	0.05	bdl	8.45	9.55	1.62	3.16
K_2O	0.01	bdl	1.33	1.40	bdl	0.02	0.29	0.23	14.84	12.29
Total	100.8	98.71	98.4	97.85	101.182	100.141	97.97	100.56	100.76	99.69
O	6	6	24	24	3	3	8	8	8	8
Si	1.996	2.003	6.853	6.813	bdl	0.001	2.853	2.826	2.989	2.983
Ti	0.004	0.005	0.164	0.173	0.954	0.961	bdl	0.001	bdl	0.001
Al	0.014	0.012	1.807	1.843	0.001	bdl	1.155	1.169	1.007	1.017
Cr	0.002	0.001	0.001	0.003	0.001	bdl	bdl	bdl	bdl	bdl
Fe	1.587	1.567	3.89	3.942	1.081	1.069	0.002	0.004	0.002	bdl
Mn	0.026	0.031	0.031	0.025	0.006	0.007	0.001	bdl	bdl	bdl
Mg	0.325	0.331	1.047	1.008	0.001	bdl	bdl	bdl	bdl	bdl
Ca	0.039	0.034	1.831	1.826	0.001	bdl	0.182	0.174	0.004	0.006
Na	bdl	0.004	0.631	0.624	0.002	bdl	0.735	0.813	0.143	0.280
K	0.001	Bdl	0.279	0.296	bdl	0.001	0.017	0.013	0.865	0.718
Total cation	3.993	3.988	16.535	16.552	2.046	2.038	4.945	5.001	5.011	5.006
An							0.195	0.174	0.004	0.006
Ab							0.787	0.813	0.142	0.279
Or							0.018	0.013	0.854	0.715
Fe_{3+}	0.000	0.000	0.776	0.8						
Fe_{2+}	1.587	1.567	3.114	3.142						
X_{Mg}	0.170	0.174	0.212	0.204						

bdl-below detection limit

Table 5: *Representative Electron Microscope Analysis of minerals in WC-10*

Mineral	**Orthopyroxene**		**Clinopyroxene**		**Ilmenite**		**Magnetite**		**Plagioclase**		**Alkalifeldspar**	
	core	**rim**	**core**	**rim**	**core**	**rim**	**core**	**rim**	**core**		**core**	**rim**
SiO_2	46.88	46.8	47.63	48.23	0	0.04	0.11	0.07	63.42	63.54	64.97	65.16
TiO_2	0.17	0.08	0.24	0.22	50.91	51.52	0.84	1.19	bdl	bdl	0.06	bdl
Al_2O_3	0.20	0.21	1.41	1.25	0.03	0.04	1.37	0.65	22.63	22.59	18.5	18.58
Cr_2O_3	0.06	bdl	bdl	bdl	bdl	bdl	0.02	0.04	0.03	bdl	bdl	bdl
FeO	48.2	46.98	27.89	27.85	45.83	46.15	91.86	92.84	0.12	0.1	0.02	0.04
MnO	2.55	2.45	1.17	1.16	2.15	2.18	0.08	0.09	bdl	0.01	bdl	bdl
MgO	1.53	1.52	1.49	1.31	0.06	0.04	0	bdl	bdl	0.01	bdl	bdl
CaO	0.81	1.97	19.31	19.05	0.01	0.01	0.01	0.01	4.23	4.18	0.12	0.37
Na_2O	0.03	0.01	0.58	0.36	0.08	0.04	0.03	bdl	9.28	9.31	2.19	3.18
K_2O	0.02	0.02	0.02	0.01	bdl	bdl	0.01	bdl	0.36	0.25	14.15	12.57
Total	100.46	100.03	99.75	99.43	99.07	100.02	94.33	94.89	100.06	99.98	100.01	99.90
O	6	6	6	6	3	3	4	4	8	8	8	8
Si	2.007	2.008	1.959	1.982	bdl	0.001	0.005	0.003	2.807	2.812	2.987	2.984
Ti	0.006	0.002	0.007	0.007	0.982	0.983	0.031	0.044	bdl	bdl	0.002	bdl
Al	0.010	0.011	0.068	0.061	0.001	0.001	0.08	0.038	1.181	1.178	1.002	1.003
Cr	0.002	bdl	bdl	bdl	bdl	bdl	0.001	0.002	0.001	bdl	bdl	bdl
Fe	1.726	1.686	0.959	0.957	0.983	0.98	3.800	3.841	0.004	0.004	0.001	0.001
Mn	0.092	0.089	0.041	0.04	0.047	0.047	0.003	0.004	bdl	bdl	bdl	bdl
Mg	0.098	0.097	0.092	0.08	0.002	0.001	bdl	bdl	bdl	0.001	bdl	bdl
Ca	0.037	0.090	0.851	0.839	bdl	bdl	0.001	0.001	0.2	0.198	0.006	0.018
Na	0.003	0.001	0.046	0.029	0.004	0.002	0.003	bdl	0.797	0.799	0.195	0.282
K	0.001	0.001	0.001	bdl	bdl	bdl	0.001	bdl	0.02	0.014	0.83	0.735
Total cation	3.983	3.985	4.024	3.995	2.019	2.016	3.925	3.933	5.01	5.005	5.023	5.023
An									0.197	0.196	0.006	0.017
Ab									0.783	0.79	0.189	0.273
Or									0.02	0.014	0.805	0.710
Fe^{3+}	0.000	0.000	0.071	0.000								
Fe^{2+}	1.726	1.686	0.888	0.957								
X_{Mg}	0.054	0.055	0.087	0.078	0.003	0.002						

bdl-below detection limit

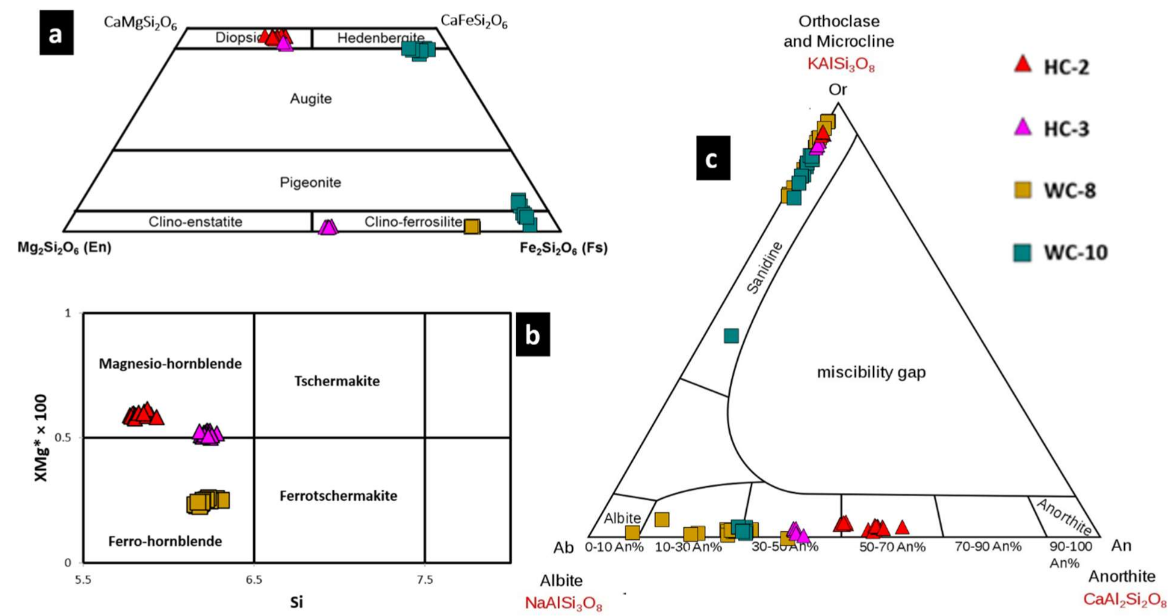

***Fig. 5:** (a) Pyroxene classification (After Morimoto, 1998), (b) Amphibolite classification, (c) Plagioclase feldspar classification (After Morimoto, 1998) for analyzed samples in HC and WC*

Orthopyroxene

Orthopyroxene compositions of analysed samples have been shown in Tables 2 and 3. The MgO content of orthopyroxene in CHCs is relatively higher (MgO wt.% 14.43-15.13 and X_{Mg} from 0.46 to 0.47) comparing those in CWCs (MgO wt.% from 1.334 to 5.422 wt.%, and the X_{Mg} from 0.049 to 0.178). Al_2O_3 content of orthopyroxene in CHCs is higher (0.5-0.8 wt.%) than those in CWCs (0.2-0.33 wt.%). In pyroxene classification (Fig. 5a), orthopyroxenes in CWCs were classified as hypersthene, whereas orthopyroxene in the sample W-10 in CHCs was classified as ferrosilite.

Clinopyroxene

The analysed sample of CHCs shows a wide range of CaO content (20.9-23.3 wt.%) compared to the CWCs (19.1-19.7 wt.%). The FeO content is low in CHCs (Fe^{2+} from 0.2 to 4.7 a.p.f.u) relative to those of the WC (Fe^{2+} from 0.9 to 1 a.p.f.u). The X_{Mg} of clinopyroxene in studied CHCs and CWCs are in the range of 0.60 - 0.68 and 0.08 - 0.15 respectively. Clinopyroxene in CHCs charnockites contains a high amount of Al_2O_3 wt.% (1.41 -4.73 wt.%) compared to CWCs (0.9-1.4 wt.%). In the pyroxene classification diagram (after Morimoto, 1989) analyzed clinopyroxene bearing charnockite in the WC side was classified as hedenbergite and those in CHCs were classified as diopside (Fig. 5a).

Hornblende

In Hornblende in CHCs, CaO ranged from (10.9-11.6 wt.%), MgO (8.3-9.5wt.%), FeO (17.7-19.6 wt.%), Al_2O_3 (10.1-13.2 wt.%) and those in CWCs, ranged (~10.3 wt.%), (3.6-4.3 wt.%), (~27-28.3 wt.%), and (9-9.8 wt.%) respectively (Tables 2 and 3). The X_{Mg} of hornblende in CHCs and CWCs are in the range of 0.45-0.48 and 0.19 - 0.21 respectively (Tables 2 and 3). The classification of amphiboles is represented in Figure 6b. In amphibolite classification, hornblende in CHCs are classified as magnesia-hornblende and those in CWCs are classified as ferro-hornblende.

Feldspars

Plagioclase in CHCs are relatively anorthite rich (An_{27-47}) compared to those in CWCs (An_{13-27}). K-feldspars in all the studied charnockites are dominantly orthoclase (Or_{71-93}). Feldspar compositions of the samples are shown in Tables 2 and 3. In contrast, the plagioclase in CHCs distribute relatively within a wide range from oligoclase to labradorite but the majority of plagioclase in CWCs are confined to oligoclase in composition (Fig. 5c).

Biotite

The composition of biotite was measured only CHCs samples (HC-3) in which biotite occurs in two textural settings as matrix biotite and overprinted biotite after orthopyroxene. Biotite in the matrix show X_{Mg} around 0.47-0.63 and Fe^{2+} is range from 0.3 to 1.2 a.p.f.u. Here, HC-3, the overprinted biotite after orthopyroxene the X_{Mg} ~0.53 and Fe^{2+} are in the range from 0.3-1 a.p.f.u.

Ilmenite and Magnetite

In CHCs, Ilmenite represents TiO_2 content in the range from 52.1-54.3 wt. % and FeO content is in the range from 43 to 45.6 wt. %. Those in CWCs vary among 50-52.4 wt. % and 45.3-51.4 wt. % respectively. The Fe^{3+} content of magnetite in CHCs is in the range from 3.9 to 4.0 a.p.f.u and those in CWCs is in the range from 3.8 to 3.9 a.p.f.u.

P-T ESTIMATION

Peak Metamorphic Condition

Using conventional thermometry

Several conventional thermometers were used to determine peak metamorphic temperature in studied charnockites. When using Fe-Mg exchange thermometers, core composition of equilibrated mineral pairs were used assuming these core compositions experience minimum resetting of Fe and Mg composition during the retrogression. The temperatures were calculations at nominal pressures of 7.5, 8, 8.5 and 9 kbars after considering the obtained pressure of the HC and WC by the previous researchers (e.g. Raase and Shenk, 1994; Hiroi et al., 1994; Hirayama et al., 2020; Dharmapriya et al., 2017, 2020)

The calculated using two-pyroxene Fe-Mg exchanged thermometer after Brey and Kohler (1990) for coexisting clinopyroxene and orthopyroxene pairs in the rocks HC-3 (CHCs) and WC-8 (CWCs) yielded average temperatures around 693, 694, 696, 697 °C and 599, 601, 604, 606 °C respectively for the considered nominal pressures. The above-calculated temperatures are considerably lower than the previously reported general metamorphic temperatures in both Highland and Wanni Complexes (Rass and Shenk, 1994; Hiroi et al., 1994; Hirayama et al., 2020; Dharmapriya et al., 2017, 2020). The two pyroxene thermometer introduced by Putirka (2008) gives reliable minimum peak metamorphic temperatures and for nominal pressure 7.5, 8, 8.5 and 9 kbars these values are ranged from 762 to 776 °C (average 769 °C), 763-777 °C (average 770 °C), 765-779 °C (average 772 °C) and 766-780 °C (average 773 °C) for HC-3s. For WC-8 at the same nominal pressures the yielded temperatures arranged from 695 to 706 °C (average 701 °C), 697-707 °C (average 702 °C), 698-708 °C (average 703 °C) and 699-710 °C (average 704 °C).

Coexisting hornblende and plagioclase core compositions of HC-3 and WC-8 were also used to determine peak metamorphic conditions using hornblende-plagioclase thermometer after Blundy and Holland (1990) and Holland and Blundy (1994). For the thermometer after Holland and Blundy (1994) the yielded average temperatures of HC-3 are in the range from 625, 631, 637 and 642 °C and for the conceded nominal. For the same nominal pressures, WC-8 yielded the average temperatures of 754, 756, 759 and 762 °C respectively. For hornblende and plagioclase after Blundy and Holland (1990), HC-3 yielded average temperatures of 665, 658, 651 and 644 °C and WC-8 yielded average temperatures of 708, 700, 693 and 685 °C respectively.

Using trace element thermometers

Pressure-independent Ti in the zircon thermometer after Ferry and Wotson (2007) was used to determine peak metamorphic conditions in CWCs (WC-28 and WC-19). Though the studied samples are SiO_2 saturated, there is no free rutile observed. However, the presence of ilmenite may suggest a relatively high TiO_2 activity at the time of zircon crystallization, assuming that the ilmenite and zircon crystallized together (Fu et al., 2008). By contrast, (Watson et al., 2006) suggested that even ilmenite-bearing rocks have been found to have TiO_2 activity as low as 0.6. According to Watson and Harrison (2005) most natural melts are capable of crystallizing zircons under the TiO_2 activities exceeding ~0.5. Therefore, we do our calculations at the TiO_2 activities exceeding 0.4 and 0.5. These calculations yielded average temperatures around 760 and 739 °C for location WC-28 and location WC-19 yields 707° and 688°C (TiO_2 activities at 0.4 and 0.5).

Retrograde metamorphic conditions

The pressure independent Ti in biotite thermometer was used to calculate overprinted biotite after pyroxene and coarse grain retrograde biotite in matrix in location HC-3. The calculated average results are 703 °C and 737 °C respectively. Yielded values represent the retrograde formation of both biotite grains in two different stages.

DISCUSSION

P-T-t Evolution of charnockites around North-eastern Part of the Inferred Boundary between the Highland and Wanni Complexes

A number of researchers have attempted to study the *P-T-t* evolution of high-grade metamorphic rocks in the HC using both metasedimentary rocks such as metapelites (Perera, 1987) and calc-silicate gneisses (e.g. Perera, 1987; Hiroi et al., 1994; Raase and Schenk, 1994; Mathavan and Fernando, 2001; Sajeev and Osanai, 2004, 2010; Dharmapriya et a., 2015a, b, 2017b) and metaigneous rocks such as metabolite (e.g Osanai et al., 2006). Due to the preservation of relict kyanite and staurolite as inclusions in porphyroblastic garnet and the presence of sillimanite both as inclusion in garnet porphyroblasts and as matrix mineral in metapelites, most of the workers suggested a clockwise trajectory for the HC granulites equilibration at peak T occurred in the sillimanite field (e.g. Perera, 1987, 1994; Hiroi et al., 1994; Raase and Schenk, 1994, Dharmapriya et al., 2017b, 2021). Although several researchers attempted to calculate the peak metamorphic *P-T* conditions in the WC rocks, there are limited studies exploring the history of *P-T* evaluation (e.g. Raase and Schenk, 1994, Hirayama et al., 2020).

Prograde Evolution

Formation of clinopyroxene and orthopyroxene via dehydration reactions (1), (2) and (3) in the HC charnockites provide evidence for prograde evolution during upper amphibolite to granulite transition (Fyfe et al., 1958; 1958; Schumacher and Faulhaber, 1994). Similar dehydration reactions have been reported from mafic granulites in the western (e.g. Dharmapriya 2015b) and the south-eastern (Perera, 1987; Schumacher and Faulhaber, 1994) part of the HC. Several researchers suggested that a stage of prograde decompression with increasing temperature for both metasedimentary (e.g. Hiroi et al., 1994, Osanai et al., 2006; Dharmapriya et al., 2015a; 2021) and metaigneous rocks (e.g. Osanai et al., 2006; Takamura et al. 2015) in the HC which represent the upper amphibolite to granulite transition of the terrine (Dharmapriya 2017b). Hence the reactions (1), (2) and (3) of the present study also probably had happened during this prograde decompression stage with increasing temperature.

Hedenbergite-Ferrosilite assemblage in WC-10 can be considered as a relict assemblage in the original igneous protolith. Dharmapriya et al. (2021) also reported the same mineral assemblage from the central part of the HC from a metadiorite. Preserved inclusion phases in porphyroblastic garnets in HC-14, which is now confirmed as an erosional remnant of WC rock lies on HC provide evidence for prograde dehydration reaction (1). Nawarathne and Perera (2015) reported sillimanite inclusion in porphyroblastic garnet in garnet-biotite gneiss and suggested that the texture is evidence for prograde evolution via the consumption of sillimanite. Formation of prograde garnet via consumption of Sillimanite-bearing assemblages (e.g. biotite+sillimanite+quartz) has been commonly reported from garnet-sillimanite-biotite-graphite gneisses (khondalites) in the HC (e.g. Hiroi et al., 1994; Rasse and Schenck, 1994; Dharmapriya et al., 2015a, 2017b). Recently Hirayama et al., (2020) attempted to determine the prograde evolution of WC via thermodynamic modelling of metapelites. Those authors suggested a stage of prograde compression up to the peak pressure conditions followed by a stage of prograde decompression with increasing temperature up to the Peak metamorphism. This prograde stage is very similar to the recently suggested prograde *P-T* path by Dharmapriya et al., 2017b) for the HC metasediments. Hence it is more reasonable to interpret that the late stage of prograde evolutions trajectory of both HC and the WC is more or less similar.

Peak metamorphic conditions

Peak metamorphic mineral assemblages observed in the northeastern part of the HC, show the coexisting primary hornblende and clinopyroxene with sharp contacts indicating peak mineral conditions (in these locations secondary hornblende grains are also identified). Hydrated minerals in anhydrous mineral assemblages are related to hornblende granulite sub-facies (Fyfe, 1958) which explain that regional mixed and intermingled assemblages generate covering the transition zone in between amphibolite to granulite facies (hornblende-granulite sub-facies to pyroxene granulite sub-facies). In contrast, a majority of studied charnockites in the WC consisted of typical anhydrous mineral assemblages during the peak metamorphic conditions representing pyroxene granulite sub-facies (Fyfe, 1958).

The estimated *P-T* conditions using Fe-Mg thermobarometer in this study represent the minimum peak metamorphic conditions due to the retrograde modification of Fe:Mg due to diffusion (e.g. Fernando et al., 2003; Pattison et al., 2003; Dharmapriya et al., 2021). Two pyroxene thermometry after Putirka (2008) gives acceptable minimum peak metamorphic temperatures of 770 °C and 700 °C for the HC and the WC respectively at nominal pressures of 8 – 9 kbar. Unfortunately studied charnockite didn't contain a suitable mineral assemblage to evaluate the pressure conditions. However, the nominal pressure conditions are more convenient since similar pressure conditions were obtained by the previous workers from the HC and the eastern margin of the WC. U-Pb zircon geochronology of the studied sample yielded Late Neoproterozoic metamorphism from 610 – 545 Ma which is consistent with the previous studies in the HC.

Retrograde evolution

A period of the near-isobaric cooling (IBC) stage after peak metamorphism has been suggested for both HC and WC gneisses. For the HC, this near-IBC stage has been suggested mainly based on fine-grain garnet formation reaction textures in mafic granulites (Perera, 1987; Schumacher et al., 1990; Pream, 1991), metapelites (Dharmapriya et al., 2015b) and calc-silicate gneisses (e.g. Mathavan and Fernando, 2001). Recently Nawarathne and Perera (2018) reported fine-grained garnet formation from metaigneous rocks close to the Eastern boundary at the central part of the WC. Garnet formation via the reaction (9) in the sample (H-W-10) in this study also provides evidence for the near-IBC stage. This is the first time report of the formation of retrograde garnets in the North-Eastern part of the WC. The perthitic texture is found in both HC (H-W-3 according to the inferred boundary) and WC (H-W-8, H-W-17, H-W-26, according to the inferred boundary) rocks. Generally, which represents retrograde isobaric cooling conditions in pelitic rocks but it is also possible to have igneous protoliths under the cooling stage therefore it is not possible to demarcate as metamorphic texture or an igneous texture (Kröner et al. 2013, Santosh et al. 2014). As well as the presence of exsolution intergrowth and twinning in clinopyroxene (H-W-27) could not be taken as a rapid cooling event due to the above reason.

The garnet breakdown via the reaction (9) indicates evidence for pressure reduction of the terrine (e.g. (Faulhaber and Raith, 1991; Schumacher and Faulhaber, 1994). Garnet breakdown in the course of decompression with oxidation has been proposed by Harley (1988) and Thost et al. (1991). In this case, the availability of oxidising fluids gneisses could have contributed to an increase in oxygen fugacity at the same time that the rocks followed the decompression path. Previously Nawarathna and Perera (2018) have reported garnet formation and breakdown reaction Kahatagaha- Kolongaha in central WC (towards the HC-WC inferred boundary). Bandara et al., (2016) reported the formation of orthopyroxene-plagioclase symplectite after garnet as evidence for decompression from a mafic block within charnockite from the northern part of the WC. Previous studies in the HC granulites inferred a stage of near Isothermal Decompression (ITD) after IBC (e.g. Perera, 1987, 1994; Mathavan and Fernando, 2001; Dharmapriya et al., 2014, 2015b) and evidence for decompression is very strong in interlayered metabasites (e.g. Schumacher and Faulhaber, 1994; Sajeev et al., 2007). However, the collected samples from the HC in this study lack evidence for garnet breakdown. White et al. (2007) suggested that mineral assemblages in dry rocks do not respond to *P-T* changes. Therefore, ITD reaction textures have not formed in most of the dry metapelitic granulites and charnockite due to a vlack of fluids/melts infiltrating through the rock after the IBC event.

As a summary, the prograde and retrograde reactions were identified during this study and these reactions give the unique direction for the metamorphic evolution of both HC and WC in the northeastern part of the Complexes. However, similar *P-T* evolution of both Complexes petrogenesis studies is not a very good tool for disclosing the tectonic boundary of the Northeastern part of the country. Except for the late Mesoproterozoic to early Neoproterozoic crystallization ages (1100 – 950 Ma) in the WC and Paleoproterozoic crystallization ages (1950-1800 Ma), rest of the crystallization ages (middle- and late- Neoproterozoic ages) itself only in metaigneous rocks cannot be taken to account to determine the tectonic boundary of the Northeastern part of the country. Because middle- and late- Neoproterozoic protolith emplacement ages has been reported in both HC and WC (e.g. Kitano et al., 2019). However, our recent geochemical investigations on charnockites of the same sampling localities (these here we have used to study metamorphic evolution) represent contrast geochemical signatures (Jayathilaka et al., 2020). Hence, the geochemical signatures of lithologies around the study area can be used as a tool to demarcate the tectonic boundary between the HC-WC.

CONCLUSIONS

Charnockites across the northeastern part of the HC-WC boundary zone of Sri Lanka represent a series of prograde to retrograde metamorphic reaction textures. Orthopyroxene of the majority of charnockites in both HC and WC was produced during the prograde dehydration of hornblende and biotite. Hedenbergite-ferrosilite assemblage in one of the charnockite in the WC can be considered as the preserved relict assemblages of its igneous protolith. Mineral assemblages and reaction textures of all the charnockites provide evidence for a clockwise pressure-temperature *(P-T)* trajectory during late prograde to retrograde evolution. Studied charnockites experienced the peak metamorphic condition with a minimum temperature of around 750- 800 °C at hornblende-granulites to pyroxene granulite facies conditions. Subsequently, these charnockites experienced a period of the near-isobaric cooling (IBC) stage.

ACKNOWLEDGEMENTS

This is a contribution to Peradeniya University Research Grant (Grant No. URG/18/43/S), and the National Research Council (NRC) Sri Lanka (grant No: NRC 19–092), PLD highly acknowledges the German Academic Exchange Service (DAAD) grant "DAAD Fellowship for Research stay for University Academics and Scientists, 2021 (grant no. 5755233). Special thanks are extended to Thilini Harischandra at NIFS, Kandy and R.K.S. Randunu, Department of Geology University of Peradeniya for their support in sample preparation.

REFERENCES

Almond, D.C. 1991. Arena Gneiss and Kandy Gneiss—a proposed subdivision of the Highland Series around Kandy, and its significance. Journal of Geological Society of Sri Lanka 3, 41–50.

Blundy, J.D., Holland, T.J. 1990. Calcic amphibole equilibria and a new amphibole-plagioclase geothermometer. Contributions to mineralogy and petrology, 104(2), pp.208-224.

Cooray, P.G. 1984. Geology, with special reference to the Precambrian. In Ecology and biogeography in Sri Lanka (pp. 1-34). Springer, Dordrecht.

Cooray, P.G. 1994. The Precambrian of Sri Lanka: a historical review. Precambrian Research, 66(1-4), pp.3-18.

Dharmapriya, P.L., Kriegsman, L.M. and Malaviarachchi, S.P. 2021. Spatial distribution of ultrahigh-temperature granulites of the Highland Complex of Sri Lanka: Lowermost continental crust above an ultrahot palaeo-Moho. Lithos, 404, p.106484.

Dharmapriya, P.L., Malaviarachchi, S.P., Galli, A., Kriegsman, L.M., Osanai, Y., Sajeev, K., Su, B.X., Tsunogae, T., Zhang, C., Adachi, T. and Dissanayake, C.B. 2021. Hybrid phase equilibria modelling with conventional and trace element thermobarometry to assess the P–T evolution of UHT granulites: An example from the Highland Complex, Sri Lanka. Journal of Metamorphic Geology, 39(2), pp.209-246.

Dharmapriya, P.L., Malaviarachchi, S.P., Galli, A., Su, B.X., Subasinghe, N.D., Dissanayake, C.B., Nimalsiri, T.B., Zhu, B. 2014. P–T evolution of a spinel+ quartz bearing khondalite from the Highland Complex, Sri Lanka: implications for non-UHT metamorphism. Journal of Asian Earth Sciences, 95, pp.99-113.

Dharmapriya, P.L., Malaviarachchi, S.P., Kriegsman, L.M., Galli, A., Dyck, B., Sajeev, K., Su, B.X. and Pitawala, A. 2020. Symplectite growth in the presence of alkaline fluids: evidence from high-aluminous metasediments of the Highland Complex, Sri Lanka. Mineralogy and Petrology, 114(6), pp.515-538.

Dharmapriya, P.L., Malaviarachchi, S.P., Kriegsman, L.M., Galli, A., Sajeev, K., Zhang, C. 2017. New constraints on the P–T path of HT/UHT metapelites from the Highland Complex of Sri Lanka. Geoscience Frontiers, 8(6), pp.1405-1430.

Dharmapriya, P.L., Malaviarachchi, S.P., Santosh, M., Tang, L., Sajeev, K. 2015. Late-neoproterozoic ultrahigh-temperature metamorphism in the Highland Complex, Sri

Lanka. Precambrian Research, 271, pp.311-333.

Dharmapriya, P.L., Malaviarachchi, S.P.K., Galli, A., Ben-Xun, Su., Subasinghe, N.D., Dissanayake, C.B. 2015a. Rare evidence for formation of garnet + corundum during isobaric cooling of UHT metapelites: new insights for retrograde P-T trajectory of the Highland Complex, Sri Lanka. Lithos 220, 300–317.

Dharmapriya, P.L., Malaviarachchi, S.P.K., Sajeev, K. and Zhang, C. 2016. New LA-ICPMS U–Pb ages of detrital zircons from the Highland Complex: insights into late Cryogenian to early Cambrian (ca. 665–535 Ma) linkage between Sri Lanka and India. International Geology Review, 58(15), pp.1856-1883.

Dharmapriya, P.L., Malaviarachchi, S.P.K., Santosh, M., Tang, L., Sajeev, K. 2015b. Late-Neoproterozoic ultrahigh temperature metamorphism in the Highland Complex, Sri Lanka. Precambrian Res. 271, 311–333.

Faulhaber, S. Raith, M. 1991. Geothermometry and geobarometry of high-grade rocks: a case study on garnet-pyroxene granulites in southern Sri Lanka. Mineralogical Magazine, 55(378), pp.33-56.

Fernando, G.W.A.R., Hauzenberger, C.A., Baumgartner, L.P., Hofmeister, W. 2003. Modeling of retrograde diffusion zoning in garnet: evidence for slow cooling of granulites from the Highland Complex of Sri Lanka. Mineralogy and Petrology, 78(1-2), pp.53-71.

Ferry, J.M., Watson, E.B. 2007. New thermodynamic models and revised calibrations for the Ti-in-zircon and Zr-in-rutile thermometers. Contributions to Mineralogy and Petrology, 154(4), pp.429-437.

Frost, B.R., Frost, C.D. 2008. A geochemical classification for feldspathic igneous rocks. Journal of Petrology, 49(11), pp.1955-1969.

Frost, B.R., Lindsley, D.H., Andersen, D.J. 1988. Fe-Ti oxide-silicate equilibria; assemblages with fayalitic olivine. American Mineralogist, 73(7-8), pp.727-740.

Frost, D.J., Mann, U., Asahara, Y.,Rubie, D.C. 2008. The redox state of the mantle during and just after core formation. Philosophical Transactions of the Royal Society A: Mathematical, Physical and Engineering Sciences, 366(1883), pp.4315-4337.

Fu, B., Page, F., Cavosie, A.J., Fournelle, J., Kita, N.T., Lackey, J.S., Wilde, S.A., Valley, J.W. 2008. Ti-in-zircon thermometry: applications and limitations. Contributions to Mineralogy and Petrology, 156(2), pp.197-215.

Fyfe WS, Turner FJ, Verhoogen J. 1958 Metamorphic reactions and metamorphic facies: Geol. Soc. America Mem.;73:259.

Harley, S.L. 1988. Proterozoic granulites from the Rauer Group, East Antarctica. I. Decompressional pressure-temperature paths deduced from mafic and felsic gneisses. Journal of Petrology, 29(5), pp.1059-1095.

He, X.F., Santosh, M., Tsunogae, T., Malaviarachchi, S.P., Dharmapriya, P.L. 2016. Neoproterozoic arc accretion along the 'eastern suture'in Sri Lanka during Gondwana assembly. Precambrian Research, 279, pp.57-80.

Hirayama, E., Tsunogae, T., Malaviarachchi, S.P., Takamura, Y., Dharmapriya, P.L., Tsutsumi, Y. 2020. Prolonged Neoproterozoic high-grade metamorphism of the Wanni Complex, Sri Lanka: New insights from petrology, phase equilibria modelling, and zircon U–Pb geochronology of partially melted cordierite gneiss from Walpita. Geological Journal, 55(9), 6147-6168

Hiroi, Y., Ogo, Y., Namba, K. 1994. Evidence for prograde metamorphic evolution of Sri Lankan pelitic granulites, and implications for the development of continental crust. Precambrian Research, 66(1-4), pp.245-263.

Holland, T., Blundy, J. 1994. Non-ideal interactions in calcic amphiboles and their bearing on amphibole-plagioclase thermometry. Contributions to mineralogy and petrology, 116(4), pp.433-447.

Hölzl, S., Hofmann, A.W., Todt, W., Krönler, H. 1994. U–Pb geochronology of the Sri Lanka basement. In: Raith, M., Hoernes, S. (Eds.), Tectonic, Metamorphic and Isotopic Evolution of Deep Crustal Rocks, With Special Emphasis on Sri Lanka. Precambrian Res., vol. 66. Precambrian Research, pp. 123–149.

Hölzl, S., Kröner, H., Kröner, A., Jaeckel, P., Liew, T.C. 1991. Geochronology of the Sri Lankan basement. In: Kröner, A. (Ed.), The Crystalline Crust of Sri Lanka, Part I.

Summary of Research of the German–Sri Lankan Consortium. Geological Survey. Department Sri Lanka, Professional. Paper 5, pp. 6–257.

Janardhan, A.S., Newton, R.C., Hansen, E.C. 1982. The transformation of amphibolite facies gneiss to charnockite in southern Karnataka and northern Tamil Nadu, India. Contributions to Mineralogy and Petrology, 79(2), pp.130-149.

Jayathilake, W. M. R., Dharmapriya, P. L., Lei, Z., Kleinschrodt, R., Kemperle, M., Spiering, B., Abewardana P., Subasinghe, N. D. (2020): Petrology geochemistry and geochronology of charnockites across the northern Highland Complex - Wanni Complex boundary, Sri Lanka. Proceedings of the 36th Technical Session of Geological Society of Sri Lanka, GSSL-2020-T1- S1/07. 2020 Published Online – 28th February 2020

Kehelpannala, K.V.W. 1991. Structural evolution of high-grade terrains in Sri Lanka with special reference to the areas around Dodangaslanda and Kandy. The crystalline crust of Sri Lanka, Part I, Summary of Research of the German-Sri Lankan Consortium. Geological Survey Department. Sri Lanka, Professional Paper, 5, pp.69-88.

Kehelpannala, K.V.W. 2003. Structural evolution of the middle to lower crust in Sri Lanka-a review. Journal of Geological Society of Sri Lanka, 11 pp. 45-85.

Kehelpannala, K.W. and Ranaweera, L.V. 2007. Structural and kinematic evolution of a possible Pan-African suture zone in Sri Lanka. In International Association of Gondwana Research Conference Series (Vol. 4, pp. 83-88).

Kehelpannala, K.W. 1997. Deformation of a high-grade Gondwana fragment, Sri Lanka. Gondwana Research, 1(1), pp.47-68.

Kehelpannala, K.W. 2004. Arc accretion around Sri Lanka during the assembly of Gondwana. Gondwana Research, 7(4S), pp.41-46.

Kitano, I., Osanai, Y., Nakano, N., Adachi, T. , Fitzsimons, I.C. 2018. Detrital zircon and igneous protolith ages of high-grade metamorphic rocks in the Highland and Wanni Complexes, Sri Lanka: their geochronological correlation with southern India and East Antarctica. Journal of Asian Earth Sciences, 156, pp.122-144.

Kleinschrodt, R., Voll, G., Kehelpannala, W. 1991. A layered basic intrusion, deformed and metamorphosed in granulite facies of the Sri Lanka basement. Geologische Rundschau, 80(3), pp.779-800.

Kriegsman, L.M. and Schumacher, J.C. 1999. Petrology of sapphirine-bearing and associated granulites from central Sri Lanka. Journal of Petrology, 40(8), pp.1211-1239.

Kriegsman, L.M. 1994. Evidence for a fold nappe in the high-grade basement of central Sri Lanka: terrane assembly in the Pan-African lower crust? Precambrian Research, 66(1-4), pp.59-76.

Kröner, A., Jaeckel, P. 1994. Zircon ages from rocks of the Wanni Complex, Sri Lanka. Journal of Geological Society of Sri Lanka, 5, pp. 41-57

Kröner, A., Williams, I.S. 1993. Age of metamorphism in the high-grade rocks of Sri Lanka. The journal of geology, 101(4), pp.513-521.

Kröner, A., Cooray, P.G., Vitanage, P.W. 1991. Lithotectonic subdivision of the Precambrian basement in Sri Lanka. In: Kröner, A. (Ed.), The Crystalline Crust of Sri Lanka, Part I. Summary of Research of the German–Sri Lankan Consortium, Geological Survey. Department Sri Lanka Professional. Paper 5, pp. 5–21.

Kröner, A., Grieling, R., Reischmann, T., Hussein, I.M., Stern, R.J., Dürr, S., Krüger, J., Zimmer, M. 1987. Pan-African crustal evolution in the Nubian segment of northeast Africa. Proterozic Lithospheric Evolution, 17, pp.235-257.

Kröner, A., Jaeckel, P., Williams, I.S. 1994. Pb-loss patterns in zircons from a high-grade metamorphic terrain as revealed by different dating methods: U□ Pb and Pb□ Pb ages for igneous and metamorphic zircons from northern Sri Lanka. Precambrian Research, 66(1-4), pp.151-181.

Kröner, A., Kehelpannala, K.V.W., Hegner, E. 2003. Ca. 750–1100 Ma magmatic events and Grenville-age deformation in Sri Lanka: relevance for Rodinia supercontinent formation and dispersal, and Gondwana amalgamation. Journal of Asian Earth Sciences, 22(3), pp.279-300.

Kröner, A., Rojas-Agramonte, Y., Kehelpannala, K.V.W., Zack, T., Hegner, E., Geng, H.Y., Wong, J., Barth, M. 2013. Age, Nd–Hf isotopes, and geochemistry of the Vijayan Complex of eastern and southern Sri Lanka: a Grenville-age magmatic arc of unknown derivation. Precambrian Res. 234, 288–321.

Liew, T.C., Milisenda, C.C., Hofmann, A.W. 1991. Isotopic contrasts, chronology of elemental transfers and high-grade metamorphism: the Sri Lanka Highland granulites, and the Lewisian (Scotland) and Nuk (SW Greenland) gneisses. Geologische Rundschau 80 (2), 279–288.

Lindsley, D.H., Frost, B.R. 1992. Equilibria among Fe-Ti oxides, pyroxenes, olivine, and quartz: Part I. Theory. American Mineralogist, 77(9-10), pp.987-1003.

Lindsley, D.H., Frost, B.R. 1992. Equilibria among Fe-Ti oxides, pyroxenes, olivine, and quartz: Part I. Theory. American Mineralogist, 77(9-10), pp.987-1003.

Madhavan, V., David, K., Mallikharjuna Rao, J., Chalapathi Rao, N.V., Srinivas, M. 1998. Comparative study of lamprophyres from the Cuddapah intrusive province (CIP) of Andhra Pradesh, India. Journal - Geological Society of India, 52, pp.621-642.

Malaviarachchi, S.P., Satish-Kumar, M., Takahashi, T. 2021. New Sr-Nd Isotope Data Record Juvenile and Ancient Crust-Mantle Melt Interactions in the Vijayan Complex, Sri Lanka. The Journal of Geology, 129(2), pp.000-000.

Mathavan, V., Fernando, G.W.A.R. 2001. Reactions and textures in grossular–wollastonite–scapolite calc–silicate granulites from Maligawila, Sri Lanka: evidence for high-temperature isobaric cooling in the meta-sediments of the Highland Complex. Lithos, 59(4), pp.217-232.

Mathavan, V.W.K.B.N., Prame, W.K.B.N., Cooray, P.G. 1999. Geology of the high grade Proterozoic terrains of Sri Lanka, and the assembly of Gondwana: An update on recent developments. Gondwana Research, 2(2), pp.237-250.

Milisenda, C.C., Liew, T.C., Hofmann, A.W., Kröner, A. 1988. Isotopic mapping of age provinces in Precambrian high-grade terrains: Sri Lanka. The Journal of Geology, 96(5), pp.608-615.

Milisenda, C.C., Liewa, T.C., Hofmanna, A.W., Köhler, H. 1994. Nd isotopic mapping of the Sri Lanka basement: update, and additional constraints from Sr isotopes. Precambrian Research, 66(1-4), pp.95-110.

Morimoto, N. 1989. Nomenclature of pyroxenes. Mineralogical Journal, 14(5), pp.198-221.

Osanai, Y., Sajeev, K., Owada, M., Kehelpannala, K.V.W., Prame, W.K.B., Nakano, N., Jayatileke, S. 2006. Metamorphic evolution of ultrahigh-temperature and high pressure granulites from Highland Complex, Sri Lanka. Journal of Asian Earth Sciences 28, 20–37.

Pattison, D.R.M. 2003. Petrogenetic significance of orthopyroxene-free garnet+ clinopyroxene+ plagioclase±quartz-bearing metabasites with respect to the amphibolite and granulite facies. Journal of metamorphic Geology, 21(1), pp.21-34.

Perera, L.R.K. 1987. Petrogenesis of granulite-facies metamorphic rocks in Sri Lanka (Doctoral dissertation).

Perera, L.R.K. 1994. PTt path vs. isotopic ages in correlations, anti-correlations, and pseudocorrelations of regional metamorphic terrains; A case study from Sri Lanka. Journal of Geological Society of Sri Lanka, 5, pp.27-41.

Pohl, J.G., Emmermann, R. 1991. Chemical composition of the Sri Lanka Precambrian Basement. In: Kröner, A. (Ed.), The Crystalline Crust of Sri Lanka, Part I. Summary of Research of the German–Sri Lankan Consortium, Geological Survey. Department Sri Lanka, Professional. Paper 5. Geological Survey Department, Sri Lanka, pp. 94–123.

Prame, W.K.B.N. 1991. Petrology of the Kataragama Complex, Sri Lanka: evidence for high P–T granulite facies metamorphism and subsequent isobaric cooling. In: Kröner, A. (Ed.), The Crystalline Crust of Sri Lanka, Part 1. Summary of Research of the German–Sri Lankan Consortium. Geol. Surv. Dept. Sri Lanka Professional Paper 5, pp. 200–224.

Putirka, K.D. 2008. Thermometers and barometers for volcanic systems. Reviews in mineralogy and geochemistry, 69(1), pp.61-120.

Raase, P., Schenk, V. 1994. Petrology of granulite-facies metapelites of the Highland

Complex, Sri Lanka: implications for the metamorphic zonation and the PT path. Precambrian research, 66(1-4), pp.265-294.

Ranaweera, L.V., Kehelpannala, K.W. 2019. Mesoscopic to microcropic structures associated with the Wanni Complex/Highland Complex Boundary Shear Zone in Sri Lanka. Journal of the Geological Society of Sri Lanka, 20(2).

Sajeev, K., Osanai, Y. 2004a. Osumilite and spinel+ quartz from Sri Lanka: Implications for UHT conditions and retrograde PT path. Journal of Mineralogical and Petrological Sciences, 99(5), pp.320-327.

Sajeev, K., Osanai, Y. 2004b. Ultrahigh-temperature metamorphism (1150 C, 12 kbar) and multistage evolution of Mg-, Al-rich granulites from the central Highland Complex, Sri Lanka. Journal of Petrology, 45(9), pp.1821-1844.

Sajeev, K., Osanai, Y., Connolly, J.A.D., Suzuki, S., Ishioka, J., Kagami, H., Rino, S. 2007. Extreme crustal metamorphism during a Neoproterozoic event in Sri Lanka: a study of dry mafic granulites. The Journal of Geology, 115(5), pp.563-582.

Sajeev, K., Williams, I.S., Osanai, Y. 2010. Sensitive high-resolution ion microprobeU–Pb dating of prograde and retrograde ultrahigh-temperature metamorphismas exemplified by Sri Lankan granulites. Geology 38, 971–974.

Santosh, M., Tsunogae, T., Malaviarachchi, S.P., Zhang, Z., Ding, H., Tang, L., Dharmapriya, P.L. 2014. Neoproterozoic crustal evolution in Sri Lanka: insights from petrologic, geochemical and zircon U–Pb and Lu–Hf isotopic data and implications for Gondwana assembly. Precambrian Research, 255, pp.1-29.

Schumacher, R., Schenk, V., Raase, P., Vitanage, P.W. 1990. Granulite facies metamorphism of metabasic and intermediate rocks in the Highland Series of Sri Lanka. In High-temperature metamorphism and crustal anatexis (pp. 235-271). Springer, Dordrecht.

Schumacher, R., Faulhaber, S. 1994. Summary and discussion of PT estimates from garnet-pyroxene-plagioclase-quartz-bearing granulite-facies rocks from Sri Lanka. Precambrian Research, 66(1-4), pp.295-308.

Shiraishi, K., Ellis, D.J., Hiroi, Y., Fanning, C.M., Motoyoshi, Y., Nakai, Y. 1994. Cambrian orogenic belt in East Antarctica and Sri Lanka: implications for Gondwana assembly. The Journal of Geology, 102(1), pp.47-65.

Takamura, Y., Tsunogae, T., Santosh, M., Malaviarachchi, S.P., Tsutsumi, Y. 2015. Petrology and zircon U–Pb geochronology of metagabbro from the Highland Complex, Sri Lanka: implications for the correlation of Gondwana suture zones. Journal of Asian Earth Sciences, 113, pp.826-841.

Takamura, Y., Tsunogae, T., Santosh, M., Malaviarachchi, S.P., Tsutsumi, Y. 2016. U–Pb geochronology of detrital zircon in metasediments from Sri Lanka: Implications for the regional correlation of Gondwana fragments. Precambrian Research, 281, pp.434-452.

Thost, D.E., Hensen, B.J., Motoyoshi, Y. 1991. Two-stage decompression in garnet-bearing mafic granulites from Sostrene Island, Prydz Bay, East Antarctica. Journal of Metamorphic Geology, 9(3), pp.245-256.

Vitanage, P.W. 1972. Post-Precambrian uplifts and regional neotectonic movements in Ceylon. Proceedings 24th IGC, pp.642-654.

Watson, E.B., Harrison, T.M. 2005. Zircon thermometer reveals minimum melting conditions on earliest Earth. Science, 308(5723), pp.841-844.

Watson, E.B., Wark, D.A., Thomas, J.B. 2006. Crystallization thermometers for zircon and rutile. Contributions to Mineralogy and Petrology, 151(4), pp.413-433.

White R.W., Powell R., Holland T.J.B. 2007. Progress relating to calculation of partial melting equilibria for metapelites. Journal of Metamorphic Geology 25:511–527